International Journal of Engineering Trends and Technology
ISSN: 2231 – 5381 /doi:10.14445/22315381/IJETT-V70I3P235

Volume 70 Issue 3, 310-318, March 2022

Original Article

Prediction and Classification of Ovarian Cancer using Enhanced Deep Convolutional Neural Network

Kokila. R. Kasture[1], Dharmaveer Choudhari[2], Pravin N. Matte[3]

[1]*Research Scholar, Department of E & TC Engineering, G H Raisoni University, Amravati, India.*
[2] *Assistant Professor, Department of E & TC Engineering, G H Raisoni College of Engineering, Nagpur, India*
[3]*Dean – Polytechnic, Department of E&TC Engineering, RSCOE, Pune, India.*

[1]kasture_kokila.ghruaphdet@ghru.edu.in

Abstract *- For the prediction and classification of Ovarian cancer's four subtypes using histopathological pictures, this article uses a deep convolutional neural network (DCNN). With a dismal survival rate, Ovarian Cancer is the fifth most common and most aggressive kind of gynecologic cancer. Serous, mucinous, endometroid, and clear cell are the four major subtypes of ovarian epithelial cancer. A new trend in medical picture analysis is the use of computers to assist in the detection of various diseases such as cancer, brain tumors, seizures, and Alzheimer's. An improved DCNN-based architecture for detecting benign and malignant cells has been developed and implemented in this paper, as shown in the figure. A subtype can be added if it is malignant. The researchers used 500 histopathological pictures from The Cancer Genome Atlas (TCGA-OV) collection, which had been made publically available, to create a total of 24,742 new images. By augmenting the photos used as training data, the proposed classification model, called KK-Net, went from 75% to 91% accuracy. This model's performance was evaluated using the AUC-ROC curve (Area under the Curve - Receiver Operating Characteristics) statistical analysis approach. An AUC-ROC curve value of 95 percent was reached on average. On top of that, we used AlexNet, VGG-16, VGG-19, and GoogleNet to test the suggested model's performance against the state-of-the-art approaches. Pathologists will be able to detect ovarian cancer in its earliest stages thanks to this newly established unique design, which can serve as a standard for predicting and classifying the disease.*

Keywords *- Artificial Intelligence, Machine learning, Predictive methods, Supervised learnings, Image processing.*

I. INTRODUCTION

The sixth-leading cause of death from cancer in women is ovarian cancer (OC). Women with OC are frequently unaware of their condition until they exhibit symptoms such as bloating, pelvic pain, weight gain, and enlargement of their abdomens [1]. However, in most cases, it is too late because the disease has spread to other parts of the body and is difficult to treat. Women's reproductive systems undergo significant structural and functional changes in the ovary over time. Menopausal women and those with OC in their families have a higher risk of developing the condition. It's difficult to catch an OC in its early stages [1]. Compared to other gynecological tumors, OC is the most common cause of death [2]. To increase the likelihood of early OC detection, numerous imaging modalities and serum indicators have been used in the study [3-5]. Biomarkers for ovarian cancer have shown great promise, but several drawbacks, such as missed detections, are time-consuming and require highly trained doctors. For the detection of Ovarian tumors, Serum Carbohydrate Antigen 125 (CA125) is one of the most commonly employed biomarkers. CA-125 concentrations may be increased in the blood of certain patients with OC in the early stages, and in the later stages, more than 80% of women [6]. Imaging methods such as ultrasound imaging, MRI, and positron emission tomography (PET) are employed in the detection and characterization of OC tumors in humans. Machine learning methods like linear support vector machine (SVM), random forest, ensemble SVM, logistic regression, or boosting [7] don't show much promise for classification accuracy. Ovarian cancer may be diagnosed earlier if a biomarker and machine learning algorithm are used together [7, 8]. [7, 8]. Early detection of ovarian cancer has been attempted in the past using supervised machine learning algorithms to classify images into either malignant or non-cancerous categories using information extracted manually. Textural and pathological features were added to a support vector machine to categorize thyroid nodules, as was done by Chen et al. [9]. Ultrasound pictures were used to detect graves' disease using SVM by Chang et al [10]. It is the goal of Jose Martinez-et Ma's al. [11] to evaluate well-known Machine Learning (ML) algorithms such as KNN, Linear Discriminant (LD), SVM, and Extreme Learning Machine (ELM) for the automatic categorization of ovarian tumors from ultrasound images. [12] Authors apply machine learning techniques like logistic regression to predict OC.

Conventional feature extraction methods rely on the manual creation of computationally complicated procedures to extract features, resulting in large dimensionality, heavy workloads, low efficiency, and poor classification rates [11-12]. Furthermore, to extract the most relevant features, a thorough understanding of

features is required during data gathering. To overcome the limits of machine learning, deep learning comes to the rescue of machine learning and can be used to process vast amounts of data [12]. One of the advantages of using deep learning algorithms is that they are capable of automatically learning raw data features.

The 15-neuron ANN model was utilized by Md. Akizur Rahman et al. to classify OCs in [13]. According to [14-15], the system cannot rely on human feature calculation in Deep learning algorithms [14-15]. The potential to analyze medical images using deep learning algorithms has attracted a large number of researchers. Various medical applications, including cancer prediction, tumor cell segmentation, illness identification, and many more [16], can benefit from recent advancements in deep learning algorithms.

DCNN was proposed by Roth et al. [17] as a method for constructing a lymph node detection system. For identifying, recognizing, and retrieving purposes, the features retrieved from images using DCNN can be useful. The non-linear network used by these deep learning methods creates a multilayer neural network for reading and extracting features. These low- and high-level features can be combined to construct an in-depth representation of incoming data and efficiently learn the dataset's key characteristics. The DCNN-based method developed by Spanhol et al. [19] has been used to classify OC based on pathological pictures. Pulmonary modules were classified using the DCNN technique by Li et al [20].
The literature showed that, even though conventional AI algorithms play an important role in the discovery of ovarian cancer, they are still not capable of meeting the standards of a pathologist's decision. Deep learning approaches have recently performed well in medical image analysis, such as thyroid nodules, breast cancer analysis, lung cancer analysis, and so on. There haven't been many studies applying deep learning in the area of ovarian cancer, and more might be done in that direction with advancements in technology. According to Wu M. and colleagues [7], their DCNN-based pre-trained AlexNet model for OC classification from histopathology pictures failed to reach an accuracy of more than 78%. There are 14 million photos over 1000 classes in ImageNet, which is used as a training dataset for state-of-the-art models such as AlexNet and VGG-Net. VGG-Net and GoogleNet appeared in 2014; AlexNet in 2012; VGG-Net and Google Net in 2013; Res Net in 2015; mobile Net and dense NET appeared in 2016; and finally, in 2017, mobile Net and dense Net were released. Most pre-trained CNN designs are based on these. Research presented in this study presents an entirely new architecture for the prediction of ovarian cancer from histopathology images using deep learning. Only histological pictures are used to train our algorithms. This architecture has a higher AUC-ROC (accuracy/precision/reliability/recall) than the other architectures studied in the literature survey. The author's contribution in this research is as follows:

- Data preparation and augmentation of histopathological images.
- Designing & implementation of Enhanced DCNN architecture, KK-net, for prediction of OC and subtype classification.
- Using Mean Square Error rate (MSE) as a cost function and activation function ELU as a substitute, an experiment in medical image analysis.
- Our model was also thoroughly tested using the most recent techniques available in the scientific community. ..

A review of earlier medical studies that utilized Deep Learning is presented in Section 1.1 of the study. Section 2 discusses the proposed methods and materials. Model evaluation metrics will be described in Section 3. Section 4 explains the proposed model's results, while Section 5 explains the general technique. Section 6 concludes the project with a conclusion.

.

II. RELATED WORK IN MEDICAL IMAGING USING DEEP LEARNING FRAMEWORK

CNN and RNN deep learning algorithms play an important role in medical image analysis, such as cancer diagnostics, predicting epilepsy, Alzheimer's diagnosis, and more [34]. Deep learning uses a variety of technologies, including Keras, Caffle, Tensorflow, Theano, and Torch [16]. Although computer vision professionals have a lack of clinical understanding and limited deep learning skills, the knowledge gap must be overcome quickly to provide satisfying results in terms of accuracy and sensitivity when dealing with biological pictures [7]. Researchers in the fields of medical image processing and deep learning have a substantial problem because of this knowledge gap. [48] Machine Learning relies on data representation rather than manually computing the features, training them, or categorizing [48]. To make the deep learning technique more shallow and efficient, it uses image pixel values directly rather than generated features from images [48].

According to Xu et al., the DCNN algorithm can be used for the classification, segmentation, and visualization of tissues in histopathology pictures. The DCNN strategy was used by Teramoto et al. [34] to classify microscopic pictures into lung cancer subtypes. Masood and colleagues built a computer-assisted decision support system to diagnose lung cancer using a deep learning approach, which yielded more accurate results. Medical imaging applications of DCNN have become more widespread and successful [7]. There are numerous uses for DCNN features collected from pictures, including recognition, identification, and retrieval [7–16]. A non-linear network is used to read and extract information from a multilayer neural network to create a deep learning architecture [7] [16] [48]. These deep learning methods combine low- and high-level features to create a representation of incoming data that is deeper than the sum of its parts. Feature extraction methods, which are often computationally

intensive in machine learning algorithms, can be reduced as a result. As a result, diagnostic systems benefit from the use of deep learning techniques. It is also true that deep learning algorithms outperform feature extraction approaches in terms of robustness. Deep Convolutional Neural Networks are used in this study to automatically identify ovarian cancer subtypes from a limited number of histopathological images.

III. MATERIALS & METHODS

A. Image Dataset

Five hundred labeled histopathological images, which included 175 serous, 100 mucinous, 60 endometroid, 80 clear-cell, and 85 non-cancerous, were retrieved from the National Cancer Institute's Genomic Data Commons data portal, TCGA-OV repository, and used for training, predicting, and further analysis in this study. Using the GDC Data Portal, researchers and bioinformaticians may easily find and download cancer-related data for further investigation. Ovarian Cancer & Subtypes Dataset Histopathology has been uploaded by the authors on the Mendeley Data website as well. [32].

B. Data Augmentation

A key activity in deep learning is the addition of new data. Data augmentation is necessary when using DCNN since a significant amount of data is needed; a huge number of images cannot always be acquired. When it's all said and done, it helps raise the database's size and add uncertainty to it. Overfitting can also be caused by insufficient training data [7] [15]. Zooming, tilting, and emphasizing certain characteristics are some of the methods used to perform this image alteration or augmentation. The original image was rotated by 90 degrees, the photographs were zoomed in to catch finer details, the images were flipped horizontally and vertically, and the brightness was boosted. An additional 24,742 photos were obtained once the photographs were enhanced, about 50 times the initial dataset's amount. JPG files of all RGB photographs were digitized in 227x227 pixel dimensions and scaled to the same dimensions. Fig. 1 depicts a variety of enhanced methods for expanding the amount of training data. One model was created for the original dataset, and the other was created specifically for the enhanced image dataset, which was around 50 times larger. The authors' data augmentation code is available on Github [33].

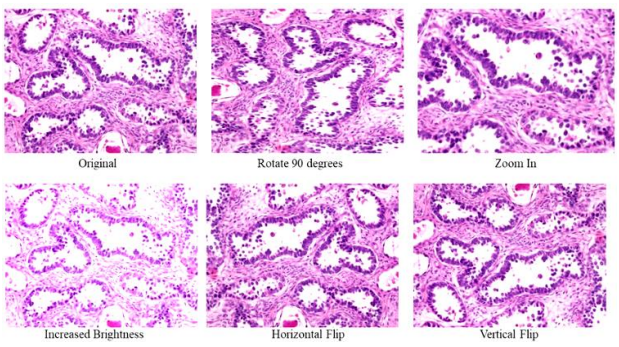

Fig. 1 Augmented histopathological images

IV. PROPOSED DCNN ARCHITECTURE (KK-NET)

Our literature study revealed that many pre-trained DCNN architectures for image classification exist, such as the AlexNet [16], VGG-Net [29], GoogleNet [30], ResNet [31], MobileNet [32] and DenseNet [33]. Inspired by these pre-trained models and the work completed by Wu M. et al. in [7], we designed and implemented an enhanced DCNN architecture with six convolutional layers, four max-pooling layers ELU as the activation function. Figure 2 illustrates the Proposed Architecture, KK-Net. We trained this model using the dataset as augmented in the above section. The primary factors considered while designing the KK-Net architecture are feature map, kernel size, stride, and activation function.

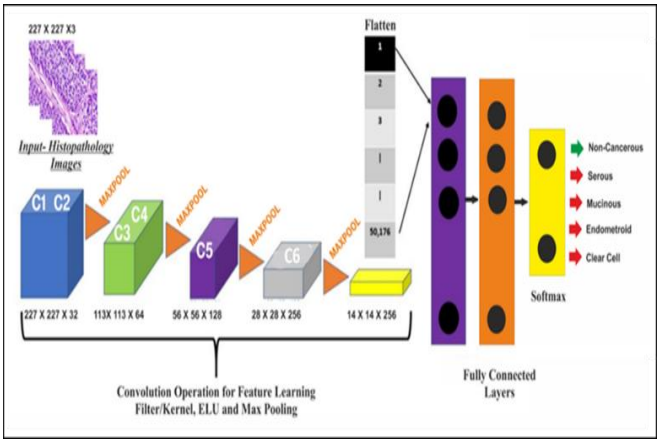

Fig. 2 Architecture of KK-Net

- The proposed model is sequentially created, layer-by-layer, & includes the convolutional, fully connected, & max-pooling layers.
- The initial two layers are convolutional layers with 32 filters and a kernel size of 3x3. Therefore, the first layer needs an input image of shape 227x227x3.
- The activation function, Exponential Linear Unit (ELU), is leveraged for all the layers other than the final output layer.
- The max-pooling layer 1 reduces dimension and considers the maximum value in the 2x2 window. Output of Maxpooling layer 1 = 113x113x32
- The third & fourth convolutional layers have 64 filters each & kernel size of 3x3 trailing with max-pooling layer 2 of window size2x2. The output of Maxpooling layer 2 = 56x56x64
- After each layer, there is an increase in the number of filters in the convolutional layer. The initial layers with fewer filters learn input images' simple features, while the deeper layers learn more complex features.
- The fifth convolutional layer with filter size 128, primarily for feature mapping, is followed by max-pooling layer 3 with a window size of 2x2. Output of Maxpooling layer 3 = 28x28x128
- The sixth and final convolutional layer is again followed by max-pooling layer 4 of 2x2 window size, further reducing overfitting. Output of Maxpooling layer 4 = 14x14x256

- The max-pooling layers' output is flattened from a three-dimensional feature map to a one-dimensional feature vector. The output of the flattened layer is connected to fully connected layers. The three fully connected layers have neuron sizes of 32, 16, and 5, respectively. The last fully-connected layer 3, has the number of neurons equivalent to the number of classes. In the present case, we have five classes, so SoftMax is set to 5.

With KK-Net, we achieved an accuracy of 91%, and it has 2,043,877 (2 million) parameters. Hyper-Parameters set for KK-Net architecture are mentioned in Table 1.

Table 1. Hyper-Parameters of KK-Net

Parameter	Value
Learning Rate	0.001
Cost function	Mean Squared Error (MSE)
Optimizer	Mean Squared Error (MSE)
Epoch Number	15
Batch Size	32
Dropout (Convolution Layer)	0.2
Dropout (Dense Layer)	0.4
Activation function	ELU

V. EXPERIMENTAL ENVIRONMENT

Nvidia T4 GPU, 16GB GPU RAM, and a 1.569GHz clock speed are used for all current research work trials at Google Collaboratory. A Windows 10 PC with 8GB RAM and an Intel Core i5-6300U CPU running at a speed of 2.40GHz and two cores are used in this example. Google Collaboratory was launched with the help of the Google Chrome web browser (GC). GC installed Google Drive storage as the host for the enhanced data. In addition, the KK-Net model is trained and tested using the Python libraries Keras and TensorFlow.

VI. PERFORMANCE EVALUATION METRICS

The performance measurements are described in detail in the following paragraph. The presented models are evaluated using several measures, such as accuracy, precision, recall, and F1-score. The confusion matrix presented above uses four values to construct these performance criteria in [21]. A deep learning method with multiple types of output can be understood using this confusion matrix. [21]. As a result, let's go over the specifics of each of these variables.

A. Accuracy: a measure based on the proportion of accurate forecasts to all of the other predictions. Mathematically, calculated as

$$Accuracy = \frac{True\ Positive + True\ Negative}{True\ Positive + True\ Negative + False\ Positive + False\ negative}$$

B. Recall: It assesses the degree to which all of the positive classifications may be reliably anticipated.

$$\text{Recall} = \frac{True\ Positive}{True\ Positive + False\ Negative}$$

C. Precision: How many forecasts were correct compared to the total number of predictions

$$\text{Precision} = \frac{True\ Positive}{True\ Positive + False\ Positive}$$

D. F1–Score: double the multiplication-and-addition of recall and accuracy ratio.

$$F1 - \text{Score} = 2 * \frac{Recall * Precision}{Recall + Precision}$$

At different thresholds, the AUC-ROC (Area under the Curve - Receiver Operating Characteristics) Curve may be used as a performance statistic. The probability curve is depicted by ROC, whereas AUC illustrates the degree to which classes may be separated Thus, the model's ability to differentiate between the classes is measured by this test. When AUC values are greater, the model is more accurate in predicting.

VII. RESULTS

An original and modified dataset was used for DCNN training and evaluation. Tenfold cross-validation was used to test its categorization accuracy. According to Table 2, the original and enhanced photos for each class are provided. Each class has roughly 5000 photos after augmentation. Figure 3 depicts the classification model's training accuracy, training loss, training accuracy, and testing accuracy, all plotted against epoch. Results of KK-measurements Net's are shown in the third table

Table 2. Number of images of each class

Class	Original Images	Augmented Images
Serous	175	5640
Mucinous	100	5223
Endometroid	60	4353
Clear Cell	80	4999
Non-Cancerous	85	4527
Total	500	24742

Table 3. Performance metrics of KK-Net

Class	Precision	Recall	F1-Score	Testing Images
ClearCell	0.88	0.94	0.91	100
Endometroid	0.96	0.96	0.96	98
Mucinous	0.89	0.91	0.91	100
Non-Cancerous	0.88	0.8	0.84	100
Serous	0.96	0.92	0.94	100

Figure 3 (A): Training Accuracy & Training Loss

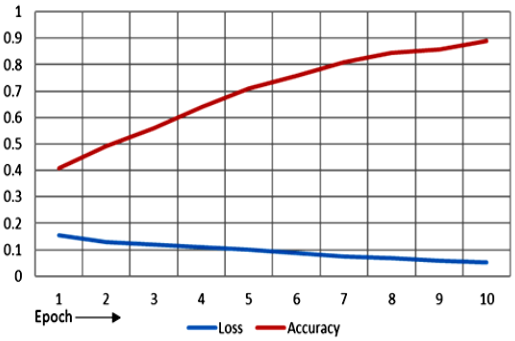

Figure 3 (B): Validation Accuracy and Validation Loss

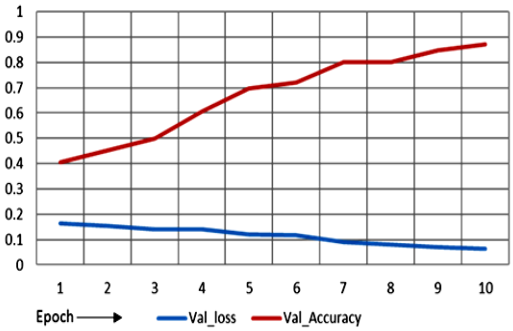

Figure 3 (C): Training Loss & Validation Loss

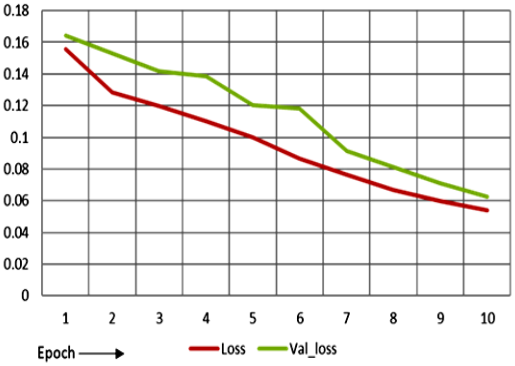

Figure 3 (D): Training Accuracy & Validation Accuracy

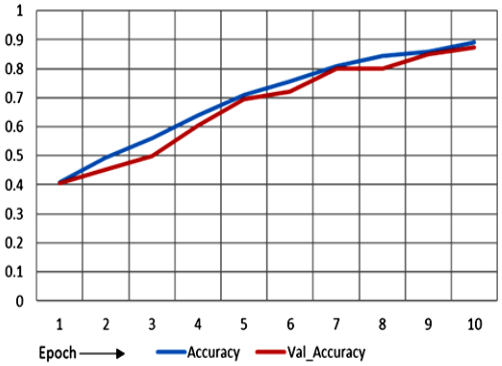

Fig. 3 Various graphs of Training & Validation accuracy & loss versus epoch | Fig. 3 (A) Training Accuracy & Loss per Epoch | Fig. 3 (B) Validation Accuracy & Loss per Epoch | Fig. 3 (C) Training & Validation Loss per Epoch | Fig. 3 (D) Training & Validation Accuracy per Epoch

Table 4. Shows the classification accuracy of the classes in scope with the original and augmented models

Class	Original Images	Augmented Images
Clear Cell	72%	84%
Endometroid	81%	92.30%
Mucinous	73%	84%
Non-Cancerous	69.79%	80%
Serous	78%	89%

Fig. 4 shows the confusion matrix of the KK-Net model's classification results, trained and tested by augmented data.

AUC-ROC is plotted for each class along with the micro-average and macro-average plots. Since AUC-ROC is usually used for binary classes, it can be extended for multi-class classification by plotting class 1 versus the rest of the classes, class 2 versus the rest of the classes, etc.

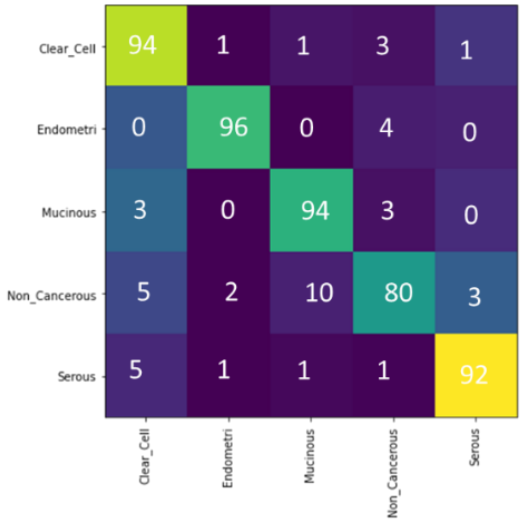

Fig. 4 Confusion Matrix of Classification results for KK-Net with an augmented dataset

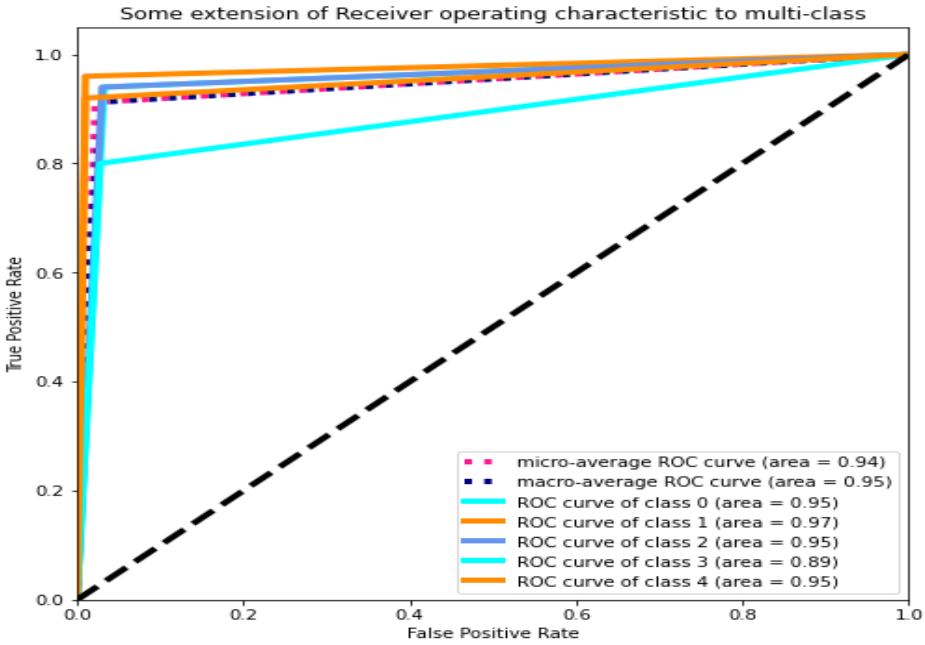

Fig. 5 AUC-ROC Curve for the KK-Net model

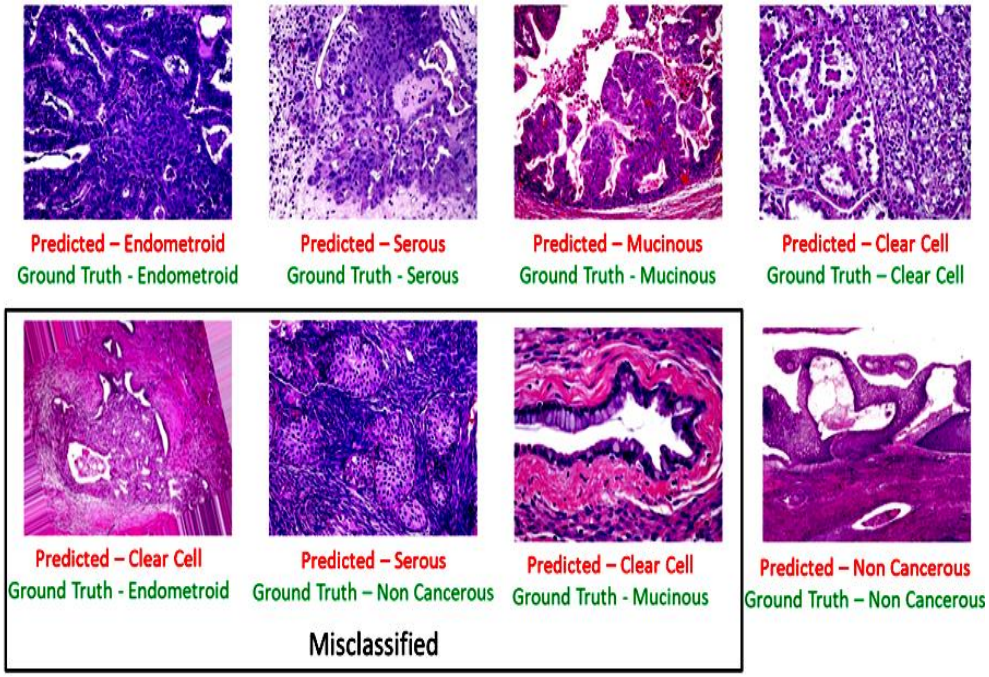

Fig. 6 Predicted and misclassified images by KK-Net

VIII. DISCUSSION

DCNN models were used instead of conventional image recognition methods to predict OC and its four subtypes from histopathology photos. To get the best results from a DCNN, it must be trained on a big dataset and generalized effectively. The original picture collection was thereby 50 times increased using rotation, zooming, horizontal and vertical reversal, brightness.

This may be observed in the training accuracy and loss per epoch shown in Fig. 3 (A), which reveals that training accuracy rose while the loss dropped. Even though the accuracy began to decline after ten epochs, we were able to end training at the best result at epoch 10. The validation accuracy began to deteriorate after epoch eight, as seen in Fig. 3 (B); as a result, a checkpoint is established and the CNN model is exported in h5 format.

Training and validation losses are shown in Fig. 3 (C), and it is expected that they will decrease as more model learning takes place (Fig. 3(C)). Zero loss is ideal, but the model requires a massive amount of data to achieve this. It was still possible to achieve near-zero losses for both the training and validation datasets, at 0.05. As shown in Fig. 3 (D), the model's training and validation accuracy follow the same path, indicating that it is capable of generalizing well.

According to Table 4 and Fig. 4, the suggested KK-Net model's classification accuracy increased from 75% to 91% for the five classes when using the expanded dataset. In [7], Wu M. et al. had reached 78.20% with a supplemented dataset, and we improved it by 12.8 percent.

We learned from Fig. 4 that training accuracy is inversely proportional to training loss, and this graph must be linear for the model to generalize successfully. In addition, as the training accuracy improved, so did the testing accuracy, reducing the likelihood of incorrect classifications in the data.

When the cost of false positives is large, precision is critical. We can't afford to label a non-cancerous picture as malignant in light of the existing problem statement. When false negatives are expensive, the recall measure becomes more important. For all classes, the KK-Net results are above 80% using the F1-Score as a counterbalance to the accuracy and recall measures. Fig. 5 shows that the KK-Net model's average performance assessment (AUC-ROC) is 95%.

Table 4 shows a 12 percent improvement in the accuracy of clear-cell classification, an 11 percent increase for endometroid, mucinous, and serious, and a 10 percent rise for non-cancerous classification. It's mostly due to the difficulty of learning the morphological properties of cells that misclassification occurs. Errors can occur because some photos are blurry or have unclear cell membranes, at times overlapping, while others have many types of carcinomas in one image. We'd like to collect a larger number of samples with poor cell morphology so that we may use that data to retrain the future research model.

We also compared our dataset to current state-of-the-art approaches, such as AlexNet, GoogleNet, VGG-16, and VGG-19, which rely on pre-trained architectures. The results obtained with these methods areas are listed in Table. 5.

Table 5. Performance Comparison of the proposed method with the state of the art Deep CNN methods

SOTA Methods	Ovarian Cancer Subtype	Precision (%)	Recall (%)	F1-Score (%)	Accuracy (%)	AUC (%)
Training-Testing Dataset Splitting for all methods: 80:20 Image Dataset Size for all methods: 24,742						
AlexNet	Clear Cell	49	78	60	72	75
	Endometroid	60	60	75		
	Mucinous	79	56	65		
	Benign	75	47	58		
	Serous	60	87	71		
VGG-16	Clear Cell	79	82	80	84	85
	Endometroid	88	87	84		
	Mucinous	80	73	76		
	Benign	82	66	78		
	Serous	63	84	72		
VGG-19	Clear Cell	87	91	95	90	93
	Endometroid	92	90	93		
	Mucinous	83	89	91		
	Benign	85	82	90		
	Serous	90	89	89		
Google-Net	Clear Cell	46	73	62	70	72
	Endometroid	59	62	61		
	Mucinous	60	59	55		
	Benign	70	57	54		
	Serous	72	63	57		
KK-Net Proposed	Clear Cell	88	94	91	91	95
	Endometroid	96	96	96		
	Mucinous	89	91	91		
	Benign	88	80	84		
	Serous	96	92	94		

In Table 5, we can see that the suggested strategy outperforms the current SOTA deep CNN methods. This is because CNN SOTA models cannot optimize model building in the cancer domain. The KK-net model, on the other hand, was created and is being utilized solely in the context of cancer research

IX. CONCLUSION

The present research is the first attempt to predict ovarian cancer and identify its four subtypes from histopathology images using a novel deep convolution neural network, KK-Net. Our model's accuracy increased from 75% to 91% with augmented images, 12.8% higher than what [7] achieved. Also, the AUC-ROC achieved is 95% for the KK-Net model, concluding that it can distinguish each class well. While designing a

DCNN, we learned that going deep does not necessarily help, and fine-tuning the hyperparameters can address many issues. Accuracy is not the only measure of performance, but the other metrics also gain importance depending on the problem statement.

We further applied our dataset to the pre-trained SOTA DCNN models, which validates the enhanced performance parameters of the proposed KK-Net model. Hence concluding that KK-Net, exclusively trained in the cancer domain, provides the optimum results for ovarian cancer prediction for multi-class.

ACKNOWLEDGMENT

The whole team at GHRU, Amravati, and Smt. Kashibai Navale College of Engineering, Pune, deserves our sincere gratitude for their unwavering support. For letting us work with Dr. Kashibai Navale and her team at Smt. Kashibai Navale Medical College on this project, we are especially grateful

REFERENCES

[1] Cancer, Who.int. [Online]. Available: www.who.int/news-room/fact-sheets/detail/cancer.

[2] Cancer.org. [Online]. Available: www.cancer.org/content/dam/cancer-org/research/cancer-facts-and-statistics/annual-cancer-facts-and-figures/2021/cancer-facts-and-figures-2021.pdf.

[3] L. A. Torre, B. Trabert, C. E. DeSantis, K. D. Miller, G. Samimi, et al., Ovarian Cancer Statistics, 2018: Ovarian Cancer Statistics, 2018, CA: A Cancer Journal for Clinicians. 68(4) (2018) 284–296.

[4] G. Chornokur, E. K. Amankwah, J. M. Schildkraut, and C. M. Phelan, Global Ovarian Cancer Health Disparities, Gynecologic Oncology. 129(1) (2013) 258–264.

[5] A. El-Nabawy, N. El-Bendary, and N. A. Belal, Epithelial Ovarian Cancer Stage Subtype Classification using Clinical and Gene Expression Integrative Approach, Procedia Computer Science. 131 (2018) 23–30.

[6] L. Zhang, J. Huang and L. Liu, Improved Deep Learning Network Based in Combination with Cost-Sensitive Learning for Early Detection of Ovarian Cancer in Color Ultrasound Detecting System, Journal of Medical Systems. 43(8) (2019) 251.

[7] M. Wu, C. Yan, H. Liu, and Q. Liu, Automatic Classification of Ovarian Cancer Types from Cytological Images using Deep Convolutional Neural Networks, Bioscience Reports. 38(3) (2018) BSR20180289.

[8] M. Shibusawa, R. Nakayama, Y. Okanami, Y. Kashikura, N. Imai, et al., The Usefulness of a Computer-Aided Diagnosis Scheme for Improving the Performance of Clinicians to Diagnose Non-Mass Lesions on Breast Ultrasonographic Images, Journal of Medical Ultrasonics. 43(3) (2016) 387–394.

[9] S. J. Chen, C. Y. Chang, K. Y. Chang, J. E. Tzeng, Y. T. Chen et al., Classification of the Thyroid Nodules Based on Characteristic Sonographic Textural Feature and Correlated Histopathology using Hierarchical Support Vector Machines, Ultrasound in Medicine and Biology. 36(12) (2010) 2018–2026.

[10] C. Y. Chang, H. Y. Liu, C. H. Tseng, and S. R. Shih, Computer-Aided Diagnosis for Thyroid Graves' Disease in Ultrasound Images, Biomedical Engineering (Singapore). 22(2) (2010) 91–99.

[11] J. Martínez-Más, A. Bueno-Crespo, S. Khazendar, M. Remezal-Solano, J. P. Martínez-Cendán, et al., Evaluation of Machine Learning Methods with Fourier Transform Features for Classifying Ovarian Tumors Based on Ultrasound Images, Plos One. 14(7) (2019) e0219388.

[12] M. Lu, Z. Fan, B. Xu, L. Chen, X. Zheng, et al., Using Machine Learning to Predict Ovarian Cancer, International Journal of Medical Informatics. 141(104195) (2020).

[13] M. A. Rahman, R. C. Muniyandi, K. T. Islam and M. M. Rahman, Ovarian Cancer Classification Accuracy Analysis using 15-Neuron Artificial Neural Networks Model, In 2019 IEEE Student Conference on Research and Development (Scored). (2019).

[14] S. Ma, L. Sigal and S. Sclaroff, Learning Activity Progression in LSTMS for Activity Detection and Early Detection, In 2016 IEEE Conference on Computer Vision and Pattern Recognition (CVPR). (2016).

[15] A. C. Costa, H. C. R. Oliveira, J. H. Catani, N. de Barros, C. F. E. Melo, et al., Data Augmentation for Detection of Architectural Distortion in Digital Mammography Using Deep Learning Approach, Arxiv [Cs.Cv]. (2018).

[16] A. Krizhevsky, I. Sutskever, and G. E. Hinton, Imagenet Classification with Deep Convolutional Neural Networks, Communications of the ACM. 60(6) (2017) 84–90.

[17] H. R. Roth, L. Lu, A. Seff, K. M. Cherry, J. Hoffman, et al., A New 2.5D Representation for Lymph Node Detection using Random Sets of Deep Convolutional Neural Network Observations, Medical Image Computing and Computer-Assisted Intervention. 17(1) (2014) 520–527.

[18] R. M. Menchón-Lara, J. L. Sancho-Gómez, and A. Bueno-Crespo, Early-Stage Atherosclerosis Detection using Deep Learning Over Carotid Ultrasound Images, Applied Soft Computing. 49 (2016) 616–628.

[19] F. A. Spanhol, L. S. Oliveira, C. Petitjean, and L. Heutte, Breast Cancer Histopathological Image Classification Using Convolutional Neural Networks, International Joint Conference on Neural Networks. (2016).

[20] W. Li, P. Cao, D. Zhao and J. Wang, Pulmonary Nodule Classification with Deep Convolutional Neural Networks on Computed Tomography Images, Computational and Mathematical Methods in Medicine. 2016 (2016) 6215085.

[21] K. Simonyan and A. Zisserman, Very Deep Convolutional Networks for Large-Scale Image Recognition, Arxiv [Cs.CV]. (2014).

[22] C. Szegedy, W. Liu, Y. Jia, P. Sermanet, S. Reed et al., Going Deeper with Convolutions, Arxiv [Cs.CV]. (2014).

[23] K. He, X. Zhang, S. Ren, and J. Sun, Deep Residual Learning for Image Recognition, Arxiv [Cs.CV]. (2015).

[24] A. G. Howard, M. Zhu, B. Chen, D. Kalenichenko, W. Wang, et al., Mobilenets: Efficient Convolutional Neural Networks for Mobile Vision Applications, Arxiv [Cs.CV]. (2017).

[25] G. Huang, Z. Liu, L. Van der Maaten and K. Q. Weinberger, Densely Connected Convolutional Networks, Arxiv [cs.CV]. (2016).

[26] K. Jung, H. Park and W. Hwang, Deep Learning for Medical Image Analysis: Applications to Computed Tomography and Magnetic Resonance Imaging, Hanyang Medical Reviews. 37(2) (2017) 61-70.

[27] I. R. Haque and J. Neubert, Deep Learning Approaches to Biomedical Image Segmentation, Informatics in Medicine Unlocked. 18 (2020) 100297.

[28] L. Guo, A. Wu, Y. Wang, L. Zhang, H. Chai, et al., Deep Learning-Based Ovarian Cancer Subtypes Identification Using Multi-Omics Data, Biodata Mining. 13(1) (2020) 10-22.

[29] R. M. Ghoniem, A. D. Algarni, B. Refky and A. A. Ewees, Multi-Modal Evolutionary Deep Learning Model for Ovarian Cancer Diagnosis, Symmetry. 13(4) (2021) 643.
[30] K. Sone, Y. Toyohara, A. Taguchi, Y. Miyamoto, M. Tanikawa, et al., Application of Artificial Intelligence in Gynecologic Malignancies: A Review Journal of Obstetrics and Gynaecology Research. 47(8) (2021) 2577-2585.
[31] Genomic Data Commons Data Portal, Cancer.gov. [Online]. Available: www.portal.gdc.cancer.gov
[32] K.Kasture, Ovarian Cancer & Subtypes Dataset Histopathology, Mendeley. (2021).
[33] (2021). K. kasture, Kokilakasture / ovarian cancer prediction, [Online]. Available: www.github.com/kokilakasture/OvarianCancerPrediction.